Research Square

Preprints are preliminary reports that have not undergone peer review.
They should not be considered conclusive, used to inform clinical practice,
or referenced by the media as validated information.

Multi-dimensional vector pixels (MDVP) for large-viewing-angle, high-resolution integral-imaging-based light field 3D displays

Huan Deng

huandeng@scu.edu.cn

Sichuan University

yuang chen

Jiangen Wu

Sichuan University

Chongji Zhao

Sichuan University

Lu Zhang

Sichuan University

Taolin Zhou

Sichuan University

Qing Qin

Sichuan University

Fushuang Wu

Sichuan University

Article

Keywords:

Posted Date: October 28th, 2026

DOI: https://doi.org/10.21203/rs.3.rs-11188327/v1

License: This work is licensed under a Creative Commons Attribution 4.0 International License.
Read Full License

Additional Declarations: There is no conflict of interest

Multi-dimensional vector pixels (MDVP) for large-viewing-angle, high-resolution integral-imaging-based light field 3D displays

Yuang Chen[1], Jiangen Wu[1], Chongji Zhao[1], Lu Zhang[1], Taolin Zhou[1], Qing Qin[1], Fushuang Wu[1], Huan Deng[1]*

[1] College of Electronics and Information Engineering, Sichuan University, Chengdu 610065, China.

*Correspondence: H. Deng, Email: huandeng@scu.edu.cn

Abstract

Restricted by the inherent space-bandwidth product of display panels, integral imaging-based light field 3D display systems suffer an inherent trade-off among multiple display performance, which severely limits their practical application. To address this issue, this paper proposes a large-viewing-angle, high-resolution integral-imaging-based light field 3D display system utilizing multi-dimensional vector pixels (MDVP). The proposed system achieves coordinated optimization of the backlight homogenization module, MDVP construction strategy, and sub-pixel overlapping mapping mechanism, enabling simultaneous improvements in viewing angle and resolution for integral imaging systems. The optimized backlight module delivers a reduced beam divergence angle and highly uniform illumination, providing a high-quality light source for 3D light field reconstruction. Different from conventional pixel units, the designed MDVP can generate multi-directional independent light fields and reconstruct complete 3D scene information via viewing zone stitching. Furthermore, a two-stage interlaced encoding scheme is adopted to rebuild the precise mapping between full-color 3D voxels and sub-pixels, effectively improving the overall system resolution. A 15.6-inch light field display prototype was developed based on the proposed method. Experimental results demonstrate that the prototype achieves a viewing angle of 64°, which is 4.5 times that of conventional integral imaging display schemes. Meanwhile, the horizontal resolution reaches 1.587 lp/mm, representing a 41.44% improvement. The proposed MDVP-based display architecture provides an effective solution to the inherent performance bottleneck of traditional integral imaging systems, exhibiting great application potential for future commercial light field 3D display products.

Introduction

Integral imaging-based light-field 3D display technology has emerged as a compelling glasses-free 3D visualization solution. It is capable of reconstructing the real-world light field distribution of 3D scenes and reproducing authentic physiological

depth cues, including accommodation cues and continuous motion parallax[1-4]. Benefiting from such superior depth presentation capability, integral imaging is widely regarded as one of the most promising technologies for next-generation 3D displays[5-9]. In practical integral imaging systems, the overall viewing experience is predominantly governed by two core performance metrics: viewing angle and 3D image quality. A broader viewing angle allows observers to perceive 3D scenes from diverse perspectives , while 3D image quality is jointly determined by resolution and depth of field. Specifically, high resolution enables precise reconstruction of object details, and an extended depth of field delivers vivid and immersive depth perception. Moreover, resolution optimization can further improve light field reconstruction accuracy, which effectively enhances depth-of-field performance and strengthens spatial depth perception. Therefore, simultaneous improvements in viewing angle and resolution are essential for upgrading the comprehensive viewing experience of integral imaging 3D displays[10,11]. Nevertheless, integral imaging systems suffer from an inherent trade-off between resolution and viewing angle, originating from the limited space-bandwidth product of display panels. For example , increasing the lens pitch expands the viewing angle but inevitably sacrifices imaging resolution. This inherent contradiction severely restricts the performance upper limit and practical deployment of integral imaging-based light field 3D display systems.

To mitigate the angle-resolution trade-off and achieve coordinated performance improvement, extensive efforts have been devoted to optimizing algorithm frameworks and innovative optical systems in recent years[12-16]. Eye-tracking-assisted light field display is a typical mainstream optimization strategy, which dynamically allocates limited display bandwidth to the user's gaze area through real-time eye position detection to enhance local image quality[17-19]. This method is applicable to single-observer scenarios and relies heavily on high-precision tracking devices, which may introduce system latency and cross-talk artifacts. Time-division multiplexing provides another feasible solution to boost light field information capacity by utilizing high-speed optical devices and human visual persistence characteristics[20-22]. As a representative branch of time-domain optimization, time-sequential backlight technology generates multi-directional dynamic illumination and cooperates with synchronized encoded images to jointly optimize viewing angle and resolution performance[23-27]. Even so, this scheme requires ultra-high-precision time synchronization among multiple components and is prone to visual flicker artifacts. In addition, spatial multiplexing adopts multi-projector array hardware to realize zone-divided images, achieving smooth and continuous motion parallax and wide viewing angle[28].

Component-level optical optimization is also an effective approach to enhance the comprehensive performance of integral imaging 3D displays. Wu et al. proposed a customized free-form backlight unit to produce highly directional and uniform illumination. Combined with an orthogonal lenticular lens array, the system constructs high-density microvoxels and realizes excellent wide-angle display performance [29].

Targeting optical aberration suppression, Xing et al. designed a three-element compound lens array and developed a two-stage geometric distortion correction algorithm. The optimized system effectively preserves high imaging quality and achieves expanded radial and circumferential field-of-view coverage [30]. In addition to hardware optimization, data-driven algorithm optimization has also been widely explored. Chang et al. established a neural-network-based light field display optimization framework, which implements global-view pre-correction for encoded images, precisely model physical display units via a dedicated display network, and further improves reconstruction accuracy with an auxiliary pre-correction network [31]. Existing studies have effectively optimized display performance by upgrading system algorithms, optical components, and hardware architectures, yet few solutions can simultaneously and efficiently break through the inherent angle-resolution bottleneck from the fundamental pixel-level encoding mechanism.

This paper proposes a high-resolution and wide-viewing-angle integral-imaging-based light field 3D display system based on multi-dimensional vector pixels (MDVP). Different from conventional pixel-based display frameworks, the proposed system adopts a systematic holistic optimization design covering multiple key modules of the light field display system. Specifically, joint optimization of a backlight homogenization module, a MDVP-based display architecture, and a two-stage interlaced sub-pixel encoding scheme is implemented to comprehensively break the traditional performance trade-off. The optimized backlight homogenization module reduces beam divergence and achieves uniform illumination, laying a high-quality optical foundation for high-fidelity 3D light field reconstruction. The newly constructed MDVP structure enables the generation of multiple independent directional light fields and realizes viewing zone stitching, which significantly expands the effective viewing angle. Furthermore, the proposed two-stage interlaced encoding scheme reconstructs the precise mapping relationship between full-color 3D voxels and display sub-pixels, effectively improving the system's spatial resolution. Benefiting from the multi-module collaborative optimization at the display sub-pixel, optical, and algorithm levels, the proposed system achieves high-fidelity light field 3D display with both high resolution and continuous wide viewing angle, providing a feasible solution for high-performance practical 3D display devices.

Results

Overall System Architecture of the MDVP-Based Display

The proposed MDVP-based light field 3D display system consists of two parts: a

customized optical hardware architecture and a dedicated light-field encoding algorithm. As illustrated in Fig. 1, the hardware platform is composed of three cascaded modules: a backlight homogenization module, an MDVP generation module, and a lenticular lens array. Specifically, the backlight homogenization module provides uniform, low-divergence illumination with controllable beam angles to support high-fidelity light-field modulation. The MDVP generation module contains an array of MDVP units, which can produce multiple independent, directionally tunable sub-light fields for multi-view reconstruction. The lenticular lens array further modulates these directional sub-light fields to form sub-viewing zones. In addition, a two-stage interlaced encoding scheme is adopted to stitch multiple sub-viewing zones and achieve seamless viewing zone stitching. Benefiting from the cooperative optimization of optical hardware and encoding strategy, the proposed system realizes high-resolution 3D imaging with a wide and continuous viewing angle.

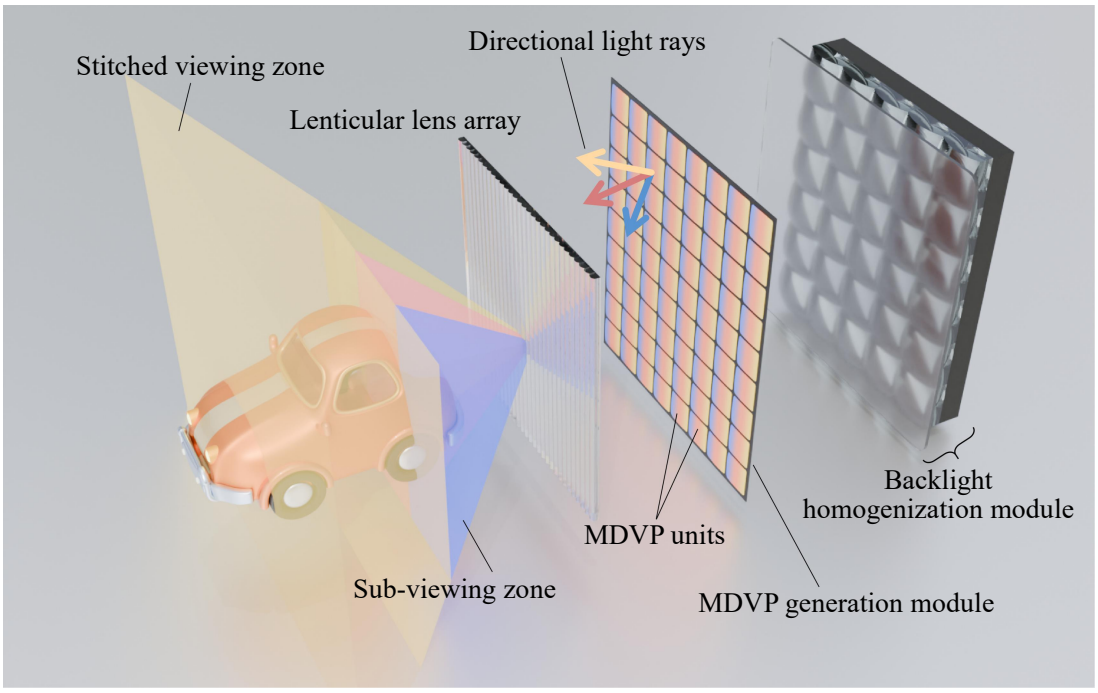

Fig. 1 Schematic of the proposed MDVP-based light field 3D display system, consisting of a backlight homogenization module, an MDVP generation module, and a lenticular lens array

Working Mechanism of Multi-Dimensional Vector Pixels (MDVP)

As shown in Fig. 2a, conventional display pixels emit omnidirectional uniform light and only record scalar light information, defined as (I_0, λ_0), where I represents light intensity and λ represents wavelength. Limited by the scalar light-emitting characteristic, traditional pixels cannot encode directional light-field information, restricting the viewing-angle expansion capability of integral imaging systems. To

address this limitation, this paper proposes a novel multi-dimensional vector pixel (MDVP) concept for high-performance light-field 3D displays. Different from conventional scalar pixels, the MDVP achieves precise modulation of directional vector light information by independently controlling the ray parameters (I_i, λ_i, θ_i) at different emission angles, where θ represents the beam propagation direction, as shown in Fig. 2b.

The MDVP unit is constructed by combining a single lenticular lens element with multiple sub-pixels, enabling angle multiplexing and directional light-field generation. According to Snell's law, light rays emitted from different sub-pixel positions produce distinct refraction angles, converting originally collimated backlight into directionally separated beam channels. The number of independent directional channels n of a single MDVP is determined by the quantity of integrated sub-pixels. As illustrated in Fig. 2c, the effective emitting area e and single-channel emission angle $\Delta\theta$ are defined as:

$$e = p_d + 2u\tan(\frac{\gamma}{2}) \tag{1}$$

$$\Delta\theta = \gamma - \frac{e}{f} \tag{2}$$

where p_d is the pixel pitch, f_M is the focal length of the lenticular lens, γ is the divergence angle of the backlight, and u is the distance between the sub-pixel plane and the principal plane of the lenticular lens. Notably, the MDVP implementation is not limited to the proposed optical configuration ; it can also be realized via micro- nano optical structures or multi- angle collimated backlight designs, exhibiting excellent structural compatibility and scalability.

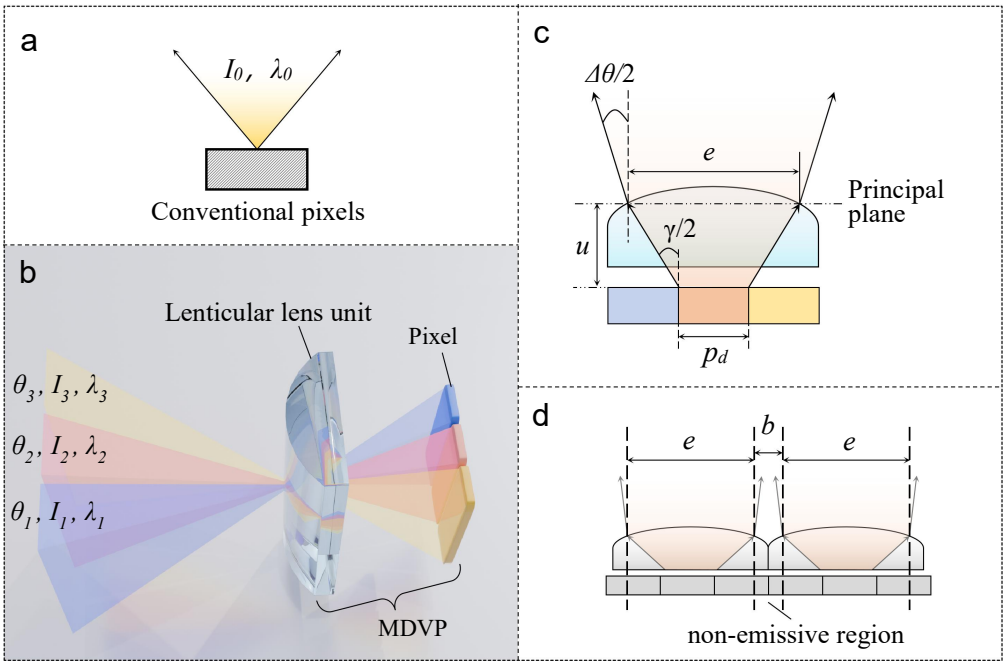

Fig. 2 Formation principle and emission characteristics of the MDVP (*n*=3). a Scalar light emission of conventional pixels. **b** Directional vector light field modulation of the MDVP. **c** Emitting area and angular characteristics of a single MDVP unit. **d** The non-emitting gaps between adjacent MDVPs

As shown in Fig. 2d, the effective light-emitting region of each MDVP only occupies a partial area of the lenticular lens element, resulting in discrete non-emitting gaps between adjacent MDVP units. These inherent blank regions lead to discontinuous 3D voxel distribution and severe imaging artifacts, degrading the final 3D display quality[32]. Our previous work has verified that voxel separation can be effectively suppressed via precise optimization of pixel emission angle[33]. Based on the geometric imaging relationship of the MDVP system, the optimal emission angle $\Delta\theta_{opt}$ for seamless voxel stitching is derived as:

$$\tan\frac{\Delta\theta_{opt}}{2}=\frac{(l-f_L)lb}{2df_L(z-l)} \tag{3}$$

where z is the 3D reconstruction depth, d is the distance between the MDVP and the lenticular lens array, l and f_L denote the image distance and focal length of the lenticular lens array, respectively, and b is the width of the non-emitting gap. To realize this optimal angular condition and eliminate voxel discontinuity, a customized backlight homogenization module is designed to precisely modulate the backlight beam divergence angle.

Design of the Backlight Homogenization Module

The backlight homogenization module consists of an LED array, a light-shielding

grating, a cemented freeform doublet array, and a diffuser, as illustrated in Fig. 3a. The light-shielding grating is adopted to isolate adjacent LED light beams and suppress lateral optical crosstalk, ensuring the independence of each illumination channel. The cemented freeform doublet array collimates the divergent LED light and preliminarily homogenizes the spatial light intensity distribution. The diffuser further fine-tunes the beam divergence angle while maintaining high spatial uniformity of the output illumination. As shown in Fig. 3b, the diffuser with a customized diffusion angle adjusts the original backlight divergence angle to the optimal value γ_{opt}. This configuration enables the MDVP to generate the optimal beam divergence angle $\Delta\theta_{opt}$, completely eliminating inter-voxel gaps and realizing seamless stitching of reconstructed 3D light fields. The quantitative relationship between γ_{opt} and $\Delta\theta_{opt}$ is given by:

$$\Delta\theta_{opt} = \gamma_{opt} - \frac{e}{f} \tag{4}$$

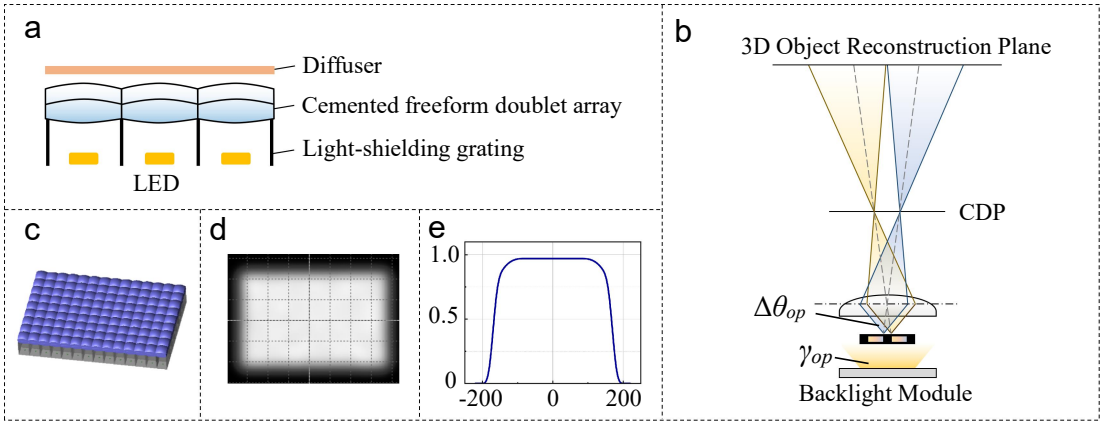

Fig. 3 Configuration and performance of the backlight homogenization module. a Optical layout. **b** Seamless beam stitching mechanism on the reconstruction plane. **c** Simulation model. **d** Simulated irradiance distribution. **e** Normalized illuminance profile of the optimized backlight

Fig.s 3c-3e show the simulation model, irradiance distribution, and normalized illuminance profile of the proposed backlight homogenization module, respectively. Simulation results demonstrate that the proposed backlight system achieves a high illumination uniformity of 92%.The optimized backlight module provides highly uniform angular and spatial illumination for all MDVP directional channels, compensating for the non-emitting defects between adjacent MDVPs and establishing a solid optical foundation for high-quality continuous viewing-zone stitching.

Mechanism of Multi-Viewing-Zone Stitching

The multi-viewing-zone stitching principle of the proposed three-channel MDVP is illustrated in Fig. 4. Benefiting from the angle-multiplexing capability of MDVP units,

each MDVP can simultaneously generate three groups of independent directional sub-light fields (I, II, and III), each carrying exclusive 3D information corresponding to a specific viewing angle. In Fig. 4a, directional rays emitted from the first sub-pixel of each MDVP are modulated by the lenticular lens array to form the first independent sub-light field (sub-light field I). Similarly, the second and third sub-pixels of each MDVP generate sub-light fields II and III, as depicted in Fig. 4b and 4c, respectively. On this basis, the proposed two-stage interlaced encoding scheme reorganizes and fuses the multi-group sub-light field information, ultimately synthesizing a complete, continuous viewing zone and reconstructing high-fidelity 3D images, as shown in Fig. 4d.

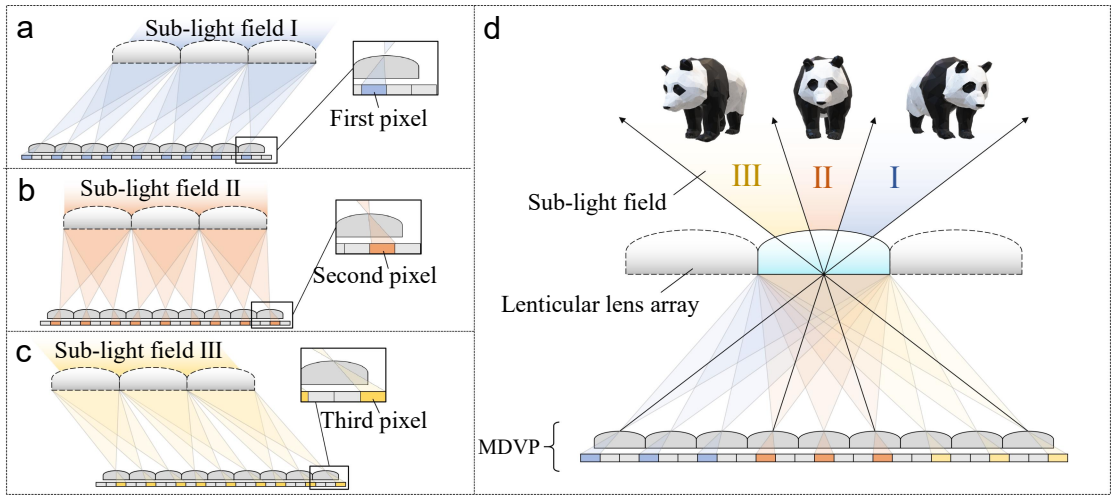

Fig. 4 Multi-viewing-zone stitching principle of the MDVP (*n*=3). a-c Generation of three independent directional sub-light field. **d** Reconstruction of a full continuous viewing zone via light field fusion

Two-Stage Interlaced Encoding Strategy

Different from the conventional integral imaging encoding mechanism that relies on scalar pixel mapping, the MDVP-based system requires a novel encoding strategy to match its vector light-field emission characteristics. Therefore, a two-stage interlaced encoding scheme is specially developed for the vector elemental image array (VEIA) generation, and the complete encoding workflow from parallax image array (PIA) to final VEIA is demonstrated in Fig. 5a.

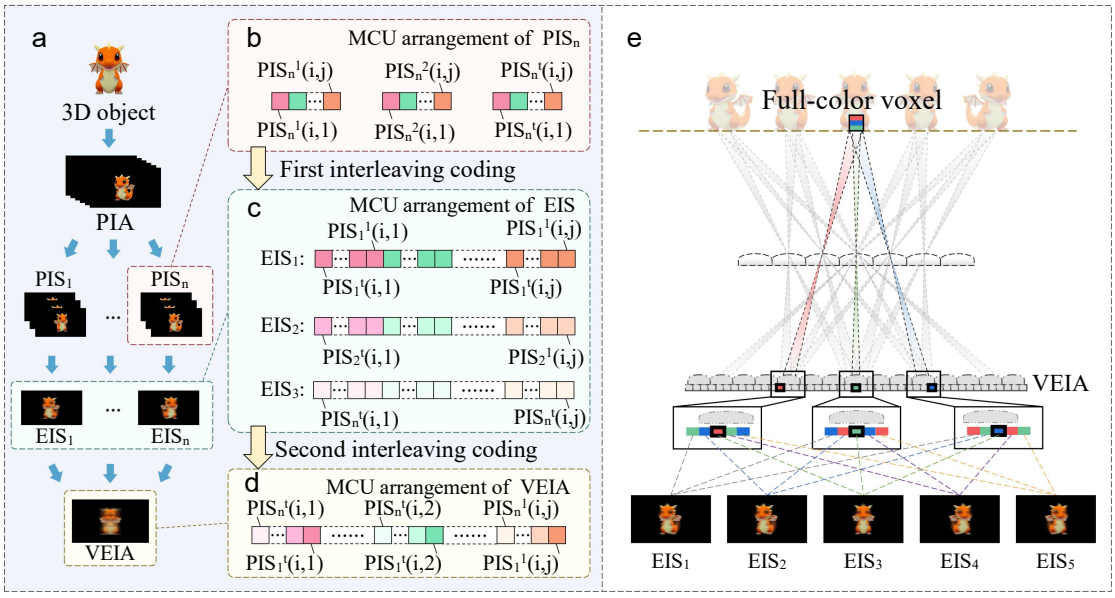

Fig. 5 Schematic diagrams related to the two-stage interlaced encoding scheme. a Workflow of the two-stage interlaced encoding scheme. **b** Arrangement of MCU in the PIS_n. **c** Arrangement of MCU in the EIS. **d** Arrangement of MCU in the VEIA. **e** Principle of 3D voxel formation in the proposed structure with the MCU as the sub-pixel

First, the original PIA containing full 3D light-field information is divided into multiple independent parallax image subarrays (PISs), denoted as PIS_1, PIS_2, ... PIS_n. Each PIS contains a sequence of parallax images indexed as PIS_n^1、PIS_n^2、... PIS_n^t. The minimum coding unit (MCU) $PIS_n^t(i,j)$ is defined as the basic encoding element, which can be a single pixel or sub-pixel to support flexible resolution optimization. The MCU arrangement within a single PIS_n is shown in Fig.5b. In the first interlacing stage, each PIS is encoded according to Eq. (5) to generate the corresponding elemental image subarray (EIS).

$$\mathrm{EIS}_n(i,j)=\begin{cases}\mathrm{PIS}_n^t\left(i,\left\lfloor\frac{j}{t}\right\rfloor+1\right) & \mathrm{mod}(j,t)=1\\ \vdots & \vdots\\ \mathrm{PIS}_n^2\left(i,\left\lfloor\frac{j}{t}\right\rfloor+1\right) & \mathrm{mod}(j,t)=t-1\\ \mathrm{PIS}_n^1\left(i,\left\lfloor\frac{j}{t}\right\rfloor\right) & \mathrm{mod}(j,t)=0\end{cases} \tag{5}$$

where $EIS_n(i,j)$ represents the MCU located at the *i-th* row and *j-th* column in the EIS_n, t denotes the total number of parallax images in each PIS, and *mod(j,t)* represents the modulo operation. The MCU distribution of the EIS is presented in Fig.5c.

In the second interlacing stage, all preprocessed EIS are further fused and encoded via Eq. (6) to generate the final VEIA.

$$\mathrm{VEIA}(i,j)=\begin{cases}\mathrm{EIS_n}(i,\left\lfloor\frac{j}{n}\right\rfloor+1) & \mathrm{mod}(j,n)=1\\ \vdots & \vdots\\ \mathrm{EIS_2}(i,\left\lfloor\frac{j}{n}\right\rfloor+1) & \mathrm{mod}(j,n)=n-1\\ \mathrm{EIS_1}(i,\left\lfloor\frac{j}{n}\right\rfloor) & \mathrm{mod}(j,n)=0\end{cases} \tag{6}$$

where VEIA*(i,j)* denotes the MCU at the *i-th* row and *j-th* column. The arrangement of MCU in the resulting VEIA is shown in Fig. 5d. As shown in Fig.5e, the proposed encoding scheme innovatively adopts sub-pixel overlapping superposition to form full-color 3D voxels. Unlike conventional displays that arrange RGB sub-pixels side-by-side to compose color voxels, the overlapping mapping mode in this work significantly reduces the physical size of single 3D voxels, effectively improving the spatial sampling rate and overall 3D imaging resolution of the system.

Performance

To experimentally verify the overall performance of the proposed MDVP-based light field 3D display, a 15.6-inch prototype has been developed, as shown in Fig.6. In this hardware implementation, sub-pixels are adopted as the MCU for the two-stage interlaced encoding scheme, and five independent directional angular-multiplexing channels are realized within each MDVP unit to expand the effective viewing angle. The detailed hardware parameters, including backlight specifications, display panel properties and lenticular lens configurations, are summarized in Table 1. For quantitative comparison, a conventional integral-imaging light field 3D display is also constructed. This reference prototype utilizes the identical commercial 2D display panel while equipping a conventional lenticular lens array with 1.52 mm lens pitch, which follows the classic integral-imaging architecture without MDVP and backlight homogenization optimization.

Table 1 Design Parameters of the Prototype

System modules		**Configuration**	**Detail**
Backlight modules		Divergence angle	7.6°
		Illumination uniformity	92%
MDVP Generation module	2D Display	Resolution	1920×1080
		Sub-pixel pitch	0.052mm

	Lenticular lens array	lens unit pitch	0.255mm
		Focal length	0.25mm
		Tilt angle	11.25°
	MDVP unit	Angular multiplex factor	5
Lenticular lens array		lens unit pitch	1.52mm
		Focal length	4mm
		Tilt angle	11.25°

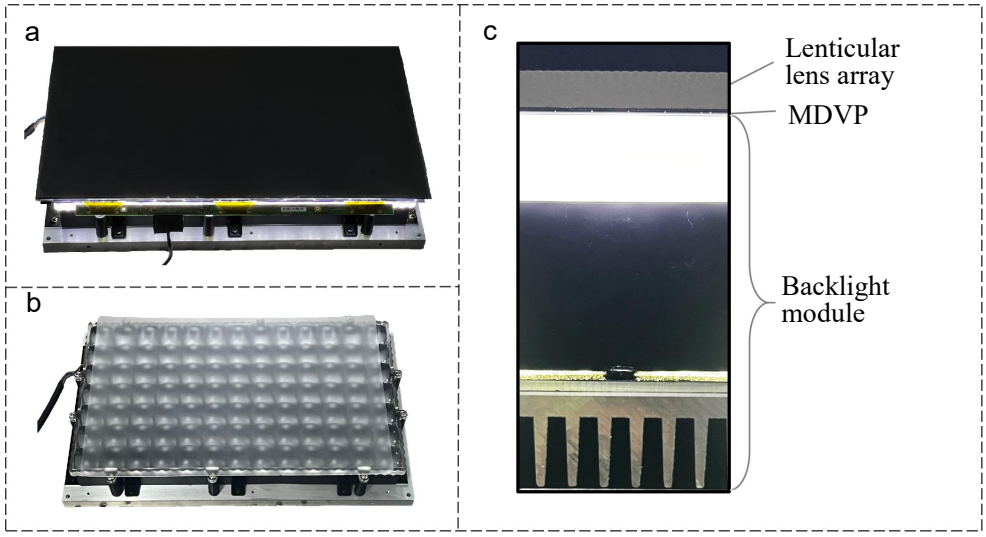

Fig. 6 Photographs of the assembled prototype and its optical-structural details. a Assembled prototype; **b** Backlight module; **c** Side-view optical structure of the prototype

Resolution is a key metric for evaluating the reconstruction capability of light field 3D displays, which reflects the system's ability to restore fine object details. The 1951 USAF resolution test chart was utilized for quantitative resolution measurement under identical experimental conditions. Fig. 7 presents side-by-side captured patterns of the resolution target from the conventional reference configuration and our proposed MDVP-based prototype.

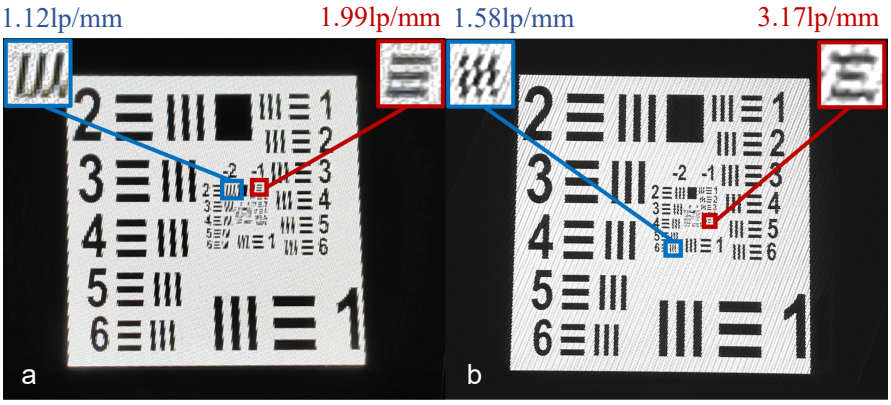

Fig. 7 Resolution comparison characterized by the 1951 USAF test chart. a conventional integral-imaging prototype; **b** proposed MDVP-based prototype

For the conventional prototype shown in Fig.7a, the measured lateral resolution is limited to Group-2 Element 2 (1.12 lp/mm), and the longitudinal resolution reaches only Group-1 Element 1 (1.99 lp/mm). Such resolution limitation originates from the inherent angle-resolution trade-off in traditional integral imaging. In comparison, benefiting from the MDVP mechanism and the two-stage interlaced sub-pixel overlapping encoding strategy, the proposed prototype achieves a lateral resolution of Group-2 Element 5 (1.58 lp/mm), representing a 41.44% enhancement. Its measured longitudinal resolution reaches Group-1 Element 5 (3.17 lp/mm), corresponding to a 59.29% improvement. Fig. 8 further illustrates the comprehensive performance comparison covering both viewing-angle and resolution metrics for the two display system.

Apart from quantitative resolution testing using standard resolution charts, 3D display experiments are carried out to intuitively evaluate the practical imaging quality of the proposed system, as shown in Fig. 8. Two 3D models with abundant surface textures and delicate contours, namely a Bronze Mask and a dragon model, are selected as test objects. In terms of the viewing-angle performance, the conventional integral-imaging prototype delivers an effective viewing angle of only 14°, which severely restricts the observer's free observation space. By contrast, benefit from the multi-viewing-zone stitching realized by MDVP angular multiplexing and the optimized backlight homogenization module, the effective viewing angle of the proposed system reaches 64°, corresponding to a 4.5-fold improvement compared with the conventional prototype. To highlight the detail-reconstruction capability, representative local regions containing rich fine features are selected for magnified observation, including the ear-eye junction of the Bronze Mask and the eye region of the dragon model. In the conventional display system (blue zoomed box), obvious

blurring can be observed at the mask's ear-eye junction, and many subtle surface textures are completely lost. Meanwhile, the eye edges of the reconstructed dragon appear jagged and coarse, caused by insufficient system sampling density. In contrast, for the proposed MDVP-based system (red zoomed box), the boundary between the eyes and ears of the Bronze Mask remains sharp, and tiny surface textures can be clearly distinguished. For the dragon model, delicate local features are well preserved, and the overall object contours are continuous and smooth without obvious aliasing artifacts.

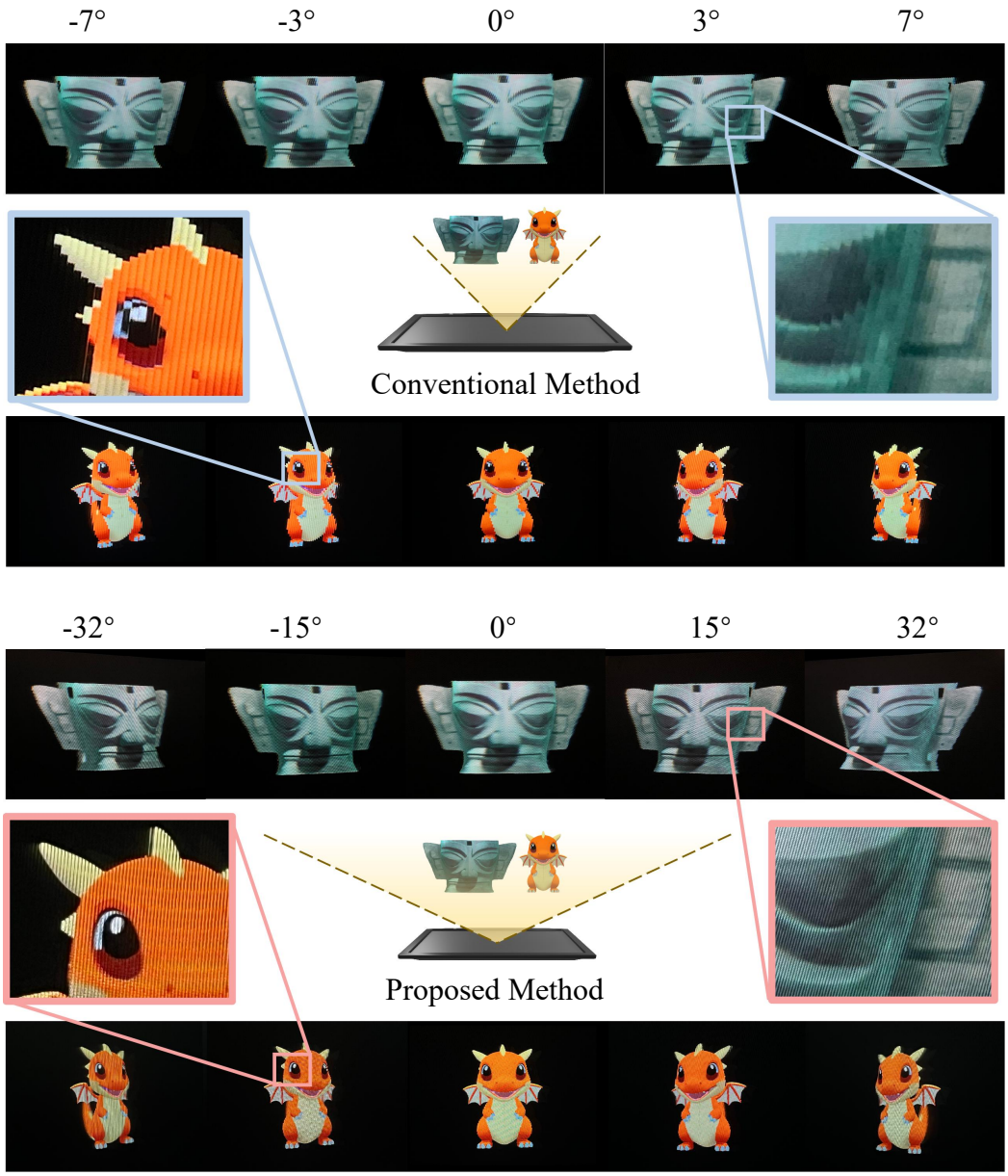

Fig. 8 Display comparison between the proposed MDVP-based scheme and the conventional integral-imaging scheme

Collectively, the experimental results demonstrate that the joint optimization of the MDVP optical architecture, backlight homogenization module and two-stage

interlaced encoding scheme effectively alleviates the intrinsic trade-off between viewing angle and resolution in integral imaging light field 3D displays. The proposed system achieves simultaneous improvement in viewing angle and 3D imaging resolution, yielding reconstructed 3D images with sharper edges and richer fine-scale textural details.

Discussion

To address the fundamental trade-off between spatial resolution and viewing angle that inherently limits the performance of integral-imaging light-field 3D displays, this work proposes and experimentally validates an MDVP-based light field 3D display approach. Instead of simply improving individual optical components, this work implements a system-level collaborative optimization strategy covering optical hardware and digital encoding algorithms. Specifically, MDVP units are constructed to produce multiple directionally independent sub-light fields through angle-multiplexing modulation. A customized backlight homogenization module is designed to precisely tune the backlight beam divergence angle, which suppresses non-emitting-region-induced voxel discontinuity and enables seamless multi-viewing-zone stitching. Meanwhile, a two-stage interlaced encoding scheme is developed to realize sub-pixel-level light field information reassignment, reducing the effective size of reconstructed 3D voxels and lifting the upper limit of system reconstruction resolution. Benefiting from the joint optimization of MDVP optical units, backlight homogenization, and interlaced encoding, the proposed system successfully achieves continuous multi-viewing-zone stitching and breaks the conventional mutual restriction between viewing angle and resolution, obtaining simultaneous improvements in both key metrics. A 15.6-inch prototype is fabricated to verify the feasibility and effectiveness of the proposed method. Quantitative characterization is conducted utilizing a 1951 USAF resolution test chart. Experimental results demonstrate that the prototype delivers a continuous viewing angle of 64°, representing a 4.5-fold enhancement relative to the conventional integral-imaging prototype. The measured lateral and longitudinal resolutions reach 1.58 lp/mm and 3.17 lp/mm, corresponding to 41.44% and 59.29% increments, respectively, compared with the reference system. The displayed 3D images confirm that the proposed system can faithfully preserve fine surface textures and subtle geometric features of 3D targets. In addition, the overall system maintains a compact form factor without requiring bulky

auxiliary optics. These merits render the MDVP-based scheme promising for practical naked-eye 3D display scenarios such as cultural heritage visualization and immersive public display. For future work, further efforts will be devoted to increasing the number of directional channels to furtherly expand the viewing angle, as well as alleviating crosstalk among adjacent MDVP units for higher-fidelity 3D reconstruction.

Methods

Numerical Simulation

In this study, the ray tracing method is adopted to conduct full-process calculation and analysis of the optical system. The luminous characteristics of LEDs are simulated as Lambertian radiation with consistent actual light intensity. The surface of the light-shielding grating is set to a full light-absorption optical property. The cemented freeform doublet array is optimized via surface iteration using optical simulation software to realize the homogenization and collimation of LED beams. The parameters of the diffusion film are configured to adjust the divergence angle of collimated beams to the optimal value γ_{opt}. For the the MDVP unit, the Jones matrix is utilized to assign polarization characteristics to sub-pixels and polarizers. The aberrations of the cylindrical-lens unit are optimized to suppress optical crosstalk and enable the MDVP unit to output the optimal emission angle $\Delta\theta_{opt}$. The irradiance distribution data of the backlight module are used to plot the normalized illuminance curve for quantitatively evaluating the illumination uniformity. The light intensity distribution data are applied to assess the beam divergence angle of the MDVP unit.

Experimental Setup

A 15.6-inch light-field 3D display prototype based on MDVP is built in an optical darkroom for experimental characterization. Meanwhile, a conventional reference prototype is constructed with a 2D display panel of the same specification. Based on the simulation optimization results, device selection and assembly of the backlight homogenization module are completed. According to the two-stage interleaved encoding scheme, the tilted cylindrical lens array is precisely matched with the display panel. The cylindrical lens array used in the experiment is fabricated via the roll-to-roll ultraviolet nanoimprint lithography process. Specifically, the roller master mold is processed by diamond turning. The UV-curable resin is coated on the PET substrate, and the microstructures are replicated by roller embossing, followed by in-situ UV

curing to yield the cylindrical lens array. A 1951 USAF resolution test target is used for quantitative characterization of system resolution. The camera is positioned 500 mm in front of the display screen to capture the target reconstruction images. The relative position between the camera and the prototype remains constant, and camera parameters are kept unchanged for both the conventional reference and proposed prototypes to guarantee consistent comparison conditions. The target reconstruction images of the MDVP prototype and the conventional reference prototype are collected respectively. The resolution index is calculated by reading the distinguishable line pair level of the target images to realize quantitative resolution comparison. In the performance test of 3D display and viewing angle, the camera is moved horizontally to acquire 3D reconstructed images at different viewing angles. Detail- feature regions of the test model are locally magnified. The edge sharpness and texture restoration performance of the two prototypes are compared to qualitatively evaluate the imaging quality of 3D light- field reconstruction.

Acknowledgements
The authors acknowledge support from the National Key Research and Development Program of China (2022YFB3606600), and the National Natural Science Foundation of China (62275179), Science and Technology Plan Projects of Tibet Autonomous Region (XZ202501ZY0066), Key Research and Development Project of Sichuan Province (2025YFRG0012).

Author details
[1]College of Electronics and Information Engineering, Sichuan University, Chengdu 610065, China

Author contributions
Y.C conceived the research idea. Y.C, J.W and C.Z carried out numerical simulations and implemented the experiments. T.Z and Q.Q completed the experimental measurements. J.W and F.W performed data analysis and provided auxiliary support for manuscript preparation. Y.C and H.D drafted the manuscript. H.D supervised the project. All authors took part in discussion of the results and provided comments on the manuscript.

Data availability
The corresponding author can provide the supporting data upon reasonable request.

Conflict of interest
The authors declare no competing interests.

References

1. Huang, H. & Hua, H. Systematic characterization and optimization of 3D light field displays. Opt. Express **25**, 18508–18525 (2017).
2. Ma, W. et al. Glasses-free 3D display with ultrawide viewing range using deep learning. Nature **648**, 76–83 (2025).
3. Wen, X. R. et al. Full-parallax high-resolution light field 3D display based on time-sequential polarization liquid crystal lens array. Light: Adv. Manuf. **7**, 069 (2026).
4. Geng, J. Three-dimensional display technologies. Adv. Opt. Photon. **5**, 456–535 (2013).
5. Wang, T. et al. Naked-eye light field display technology based on mini/micro light emitting diode panels: a systematic review and meta-analysis. Sci. Rep. **14**, 24381 (2024).
6. Zhang, Z. et al. High-fidelity light-field display with enhanced information utilization by modulating chrominance and luminance separately. Light Sci. Appl. **14**, 78 (2025).
7. Fan, Z. B. et al. Integral imaging near-eye 3D display using a nanoimprint metalens array. eLight **4**, 3 (2024).
8. Hua, J. et al. Foveated glasses-free 3D display with ultrawide field of view via a large-scale 2D-metagrating complex. Light Sci. Appl. **10**, 213 (2021).
9. Bai, Y. C. et al. Sub-pixel marking and depth-based correction methods for the elimination of voxel drifting in integral imaging display. Opt. Express **32**, 12243–12256 (2024).
10. Ma, H. et al. Parameter optimization method for light field 3D display. Opt. Express **31**, 42206–42217 (2023).
11. Pei, X. et al. Three-dimensional light field fusion display system and coding scheme for extending depth of field. Opt. Lasers Eng. **169**, 107716 (2023).
12. Liu, Z. S. et al. Integral imaging-based light field display system with optimum voxel space. IEEE Photonics J. **16**, 1–7 (2024).
13. Hua, J. et al. Recent Advances in Planar Optics-Based Glasses-Free 3D Displays. Front. Nanotechnol. **4**, 829011 (2022).
14. Li, C. et al. Viewing angle enhancement for integral imaging display using two overlapped panels. Opt. Express **31**, 21772–21783 (2023).
15. Xia, X. et al. Moiré-free and high-resolution light field 3D display based on random parallax barrier. J. Phys.: Photonics **7**, 035009 (2025).
16. Liu, Y. J. et al. High-Resolution Integral Imaging Display Using Targeted Optimized Compound Lens Array for Voxel Aliasing Elimination. Laser Photonics Rev. **18**, 2400182 (2024).
17. Li, X. et al. Multi-user, high-resolution, high-quality directional backlight autostereoscopic display. Opt. Commun. **520**, 128456 (2022).
18. Xiong, Z. L. et al. Partially-overlapped viewing zone based integral imaging system with super wide viewing angle. Opt. Express **22**, 22268–22277 (2014).
19. Dorado, A. et al. Toward 3D integral-imaging broadcast with increased viewing

angle and parallax. Opt. Lasers Eng. **107**, 83–90 (2018).
20. Wang, X. & Hua, H. Time-multiplexed method for view density enhancement in integral imaging-based light field displays. Opt. Lett. **47**, 4471–4474 (2022).
21. Kim, Y. et al. Point light source integral imaging with improved resolution and viewing angle by the use of electrically movable pinhole array. Opt. Express **15**, 18253–18267 (2007).
22. Chen, Y. F. et al. Super-Snell scanning light-field display for ultrawide-angle high-resolution glasses-free three-dimensional displays. Nat. Photon. https://doi.org/10.1038/s41566-026-01938-8 (2026).
23. Ma, S. et al. Enhancing integral imaging performance using time-multiplexed convergent backlight. Appl. Opt. **59**, 3165–3173 (2020).
24. Zhuang, X. et al. High-resolution integral imaging 3D display using time-multiplexed directional backlight. Opt. Express **34**, 6624–6635 (2026).
25. Yang, L. et al. Viewing-angle and viewing-resolution enhanced integral imaging based on time-multiplexed lens stitching. Opt. Express **27**, 15679–15692 (2019).
26. Liu, B. et al. Time-multiplexed light field display with 120-degree wide viewing angle. Opt. Express **27**, 35728–35739 (2019).
27. Hua, J. et al. Time-multiplexed vector light field display with intertwined views via metagrating matrix. Opt. Lasers Eng. **164**, 107527 (2023).
28. Yu, X. et al. Dynamic three-dimensional light-field display with large viewing angle based on compound lenticular lens array and multi-projectors. Opt. Express **27**, 16024–16031 (2019).
29. Zhang, Z. et al. Miniaturized-voxel light field panel display based on an ultra-slim and large-area freeform directional backlight. Optica **12**, 1632–1639 (2025).
30. Xing, Y. et al. Integral imaging-based tabletop light field 3D display with large viewing angle. Opto-Electron. Adv. **6**, 220178 (2023).
31. Chang, J. et al. Display performance optimization method for light field displays based on a neural network. Opt. Express **32**, 19265–19278 (2024).
32. He, Y. et al. Harnessing the plenoptic function for a directionally illuminated autostereoscopic display. Opt. Express **30**, 45553–45568 (2022).
33. Zhao, C. J. et al. Integral imaging three-dimensional display system with anisotropic backlight for the elimination of voxel aliasing and separation. Opt. Express **31**, 29132–29144 (2023).